ELSEVIER

Thermochimica Acta 307 (1997) 27–35

thermochimica acta

A new method for the analysis of non-isothermal DSC and diffraction data

J.A. Kennedy, S.M. Clark*

Synchrotron Radiation Department, Daresbury Laboratory, Daresbury, Warrington, Cheshire WA4 4AD, UK

Received 18 December 1995; accepted 29 February 1996

Abstract

A general method for the analysis of non-isothermal kinetic data is presented. The method is suitable for the analysis of data collected using time resolved powder diffraction and differential scanning calorimetry. The problems associated with previous methods are outlined and the new expression derived. An implementation strategy is also presented. The method is illustrated with the analysis of data collected as part of a real-time study of the I→II phase transition in NH_4Cl. Energies of activation of 400(80) and 450(90) kJ/mol were obtained for this transformation using time resolved powder diffraction and differential scanning calorimetry, respectively. © 1997 Elsevier Science B.V.

Keywords: Ammonium halides; Calorimetry; Kinetics; Powder diffraction; Time resolved

1. Introduction

Industrial furnacing provides the primary route to most of the materials that we use in our everyday lives. The study of the kinetics of these processes provides rate equations, which are needed for the design of pilot or full scale production plants, and parameters such as the activation energy, which allow different processes or different reaction conditions to be compared. This can aid in the optimisation of existing processes and the development of new processes and synthesis routes.

Time resolved powder diffraction (TRPD) and differential scanning calorimetry (DSC) are the two techniques that are most frequently used to study the kinetics of solid state phase transitions and chemical reactions that involve solid components. For both TRPD and DSC, two methods of data collection are commonly used: the isothermal method and the non-isothermal method.

The isothermal method involves heating or cooling the system under study to a temperature past the reaction onset temperature and then monitoring the reaction at that fixed temperature. This approach has the advantage that the methods of data analysis are well established [1] but suffers from the disadvantages that: multiple measurements are required, knowledge of the reaction onset temperature is necessary before measurements can be made and it is not always possible to heat the sample to the required reaction temperature before the reaction has commenced.

The non-isothermal method involves heating or cooling the sample at a constant rate to a temperature well beyond the reaction temperature while monitoring the reaction. This avoids the experimental problems associated with the isothermal method. In some cases one non-isothermal measurement can give as

*Corresponding author. Tel.: +44 0 1925 603123; fax: +44 0 1925 603124.

PII S0040-6031(96)02962-0

much information as a series of isothermal measurements and therefore offers a much more efficient data collection route. For this reason many methods for the analysis of non-isothermal data have been proposed and the results of a large number of kinetic studies using the non-isothermal method have been reported. Unfortunately, the existing methods for the analysis of data collected under non-isothermal conditions are inappropriate for the majority of reactions and transformations. This makes it impossible to compare reported values determined using different methods.

We here present a general method for the analysis of non-isothermal kinetic data which is free from any assumptions, can be used with any rate equation and to analyse data collected using both TRPD and DSC. The method is demonstrated with an analysis of DSC and TRPD data collected as part of a non-isothermal study of the I→II phase transition in ammonium chloride.

Table 1
Common forms of integrated rate equation

Acceleratory rate equations	
Power law	$f(\alpha)=\alpha^{1/m}$
Exponential law	$f(\alpha)=\ln\alpha$
Sigmoid rate equations	
Avrami	$f(\alpha)=[-\ln(1-\alpha)]^{1/n}$
Prout–Tomkins	$f(\alpha)=\ln[\alpha/(1-\alpha)]$
Deceleratory rate equations	
One-dimensional diffusion	$f(\alpha)=\alpha^2$
Two-dimensional diffusion	$f(\alpha)=(1-\alpha)\ln(1-\alpha)+\alpha$
Three-dimensional diffusion	$f(\alpha)=[1-(1-\alpha)^{1/3}]^2$
Geometric models	
Contracting area	$f(\alpha)=1-(1-\alpha)^{1/2}$
Contracting volume	$f(\alpha)=1-(1-\alpha)^{1/3}$

Note: The shape factors m and n are usually integer or half integer and depend upon the mechanisms and dimensionality of nucleation and growth.

2. Theoretical background

Integrated rate equations can be written generically in the form [1]:

$$f(\alpha) = kt \tag{1}$$

where α is the degree of reaction, k is the reaction rate, t is the elapsed time since the start of the reaction and f is a function that relates the degree of reaction to the product kt. Some commonly used expressions are contained in Table 1 [1].

The reaction rate is temperature dependant and can usually be calculated from the Arrhenius equation [2]:

$$k = A\exp(-E/RT) \tag{2}$$

Here, T is the absolute temperature, R is the molar gas constant, E is the overall effective activation energy of the reaction and A is a constant, known as the pre-exponential factor, that defines the maximum possible value of k.

Non-isothermal experiments take place under conditions of constantly ramping temperature. If we define T_0 as the temperature at the start of the reaction and b as the time rate of temperature increase, then the temperature at time t is given by:

$$T = bt + T_0 \tag{3}$$

Eqs. (1)–(3) can be combined in a number of ways to give expressions relating the degree of reaction to the activation energy. Such expressions form the basis of the current methods of non-isothermal data analysis. The most commonly used of these methods are those proposed by Kissinger [3], Augis and Bennett [4], Takhor [5], and Coats, Redfern [6], Sestak [7] and Satava [8]. All of these methods were developed using simplifying assumptions that limit their applicability:

1. All of these methods, except for that of Coats, Redfern, Sestak and Satava, were derived specifically in terms of the Avrami equation [9–13] and are not applicable to a general rate equation.
2. The methods of Kissinger, Augis and Bennett, Coats, Redfern, Sestak and Satava assume that T_0 is negligibly small compared with T. This assumption introduces a substantial error for reactions that take place well above absolute zero.
3. All of the methods except that of Augis and Bennett ignore the temperature dependence of k during differentiation of the Avrami equation.
4. The scope of application of the methods of Coats, Redfern, Sestak and Satava and Augis and Bennett is limited by assumptions concerning the size of the activation energy and associated quantities.

Other methods have been proposed [1,14], but none are generally applicable or assumption free.

3. New method of analysis

Inspection of Eqs. (1)–(3) reveals that they can be combined to give an expression that is generally applicable. Firstly, Eq. (1) can be rearranged to give:

$$k = \frac{f(\alpha)}{t} \tag{4}$$

then, equating this with Eq. (2) gives:

$$\frac{f(\alpha)}{t} = Ae^{-(E/RT)} \tag{5}$$

and then Eq. (3) can be used to substitute temperature for time dependence which gives:

$$\frac{bf(\alpha)}{(T - T_0)} = Ae^{-(E/RT)} \tag{6}$$

taking logarithms of both sides of this equation gives:

$$\ln\left[\frac{bf(\alpha)}{(T - T_0)}\right] = \ln(A) - \frac{E}{RT} \tag{7}$$

Plotting the left-hand side of this equation against $1/T$ should give a straight line of gradient $-E/R$ and intercept $\ln(A)$. This is the non-isothermal equivalent of an Arrhenius plot [1] and will be referred to as a ln–ln plot throughout the rest of this text. Eq. (7) can incorporate any rate equation and is free from any of the assumptions used to derive previous expressions but, surprisingly, has not been previously proposed as a basis for the analysis of non-isothermal kinetic data.

Some rate equations have an extra parameter, in addition to the rate constant k, which is usually also a constant with respect to temperature and time. Two such rate equations are the Avrami and power law equations which contain the parameters n and m, respectively (Table 1). Such equations can be written in the form $f(\alpha)=g(\alpha)^p$, where p is the unknown constant and g is some function of α. After re-arranging Eq. (7) and multiplying by a constant q, we obtain:

$$\ln[f(\alpha)^q] = q\left[\ln(A) - \frac{E}{RT}\right] + q\ln\left(\frac{T - T_0}{b}\right) \tag{8}$$

then by setting q equal to the reciprocal of p this becomes:

$$\ln[g(\alpha)] = \frac{1}{p}\left[\ln(A) - \frac{E}{RT}\right] + \frac{1}{p}\ln\left(\frac{(T - T_0)}{b}\right) \tag{9}$$

Since the quantity $[\ln(A)-E/RT]/p$ is constant for any particular value of T, a plot of $\ln[g(\alpha)]$ versus $\ln[(T-T_0)/b]$ will have gradient $1/p$. For example, for the Avrami equation, putting $g(\alpha)=\ln[-(\ln(1-\alpha))]$ will yield a plot with gradient n and for a power law rate equation, a plot with gradient m will result from making $g(\alpha)=\ln(\alpha)$. So any extra parameters can be found by making a series of measurements at different heating rates and then selecting the value of the fraction transformed corresponding to a chosen temperature from each of the measurements made. The temperatures at which the values of the fraction transformed are selected are most sensibly chosen so that each value is non-zero. Values of the fraction transformed can be selected at more than one temperature; this gives a number of estimates of the parameter p. For the case of the Avrami equation this method is equivalent to the method proposed by Ozawa [15] for determining n but without the assumption that T_0 is independent of heating rate since T_0 is explicitly included in Eq. (9).

For powder diffraction studies the degree of reaction can be obtained directly from normalised TRPD peak intensities. DSC data consists of measurements of heat flow, Δq, which is proportional to the rate of transformation. Normalised DSC data must be integrated with respect to time in order to obtain the degree of reaction. This can be done, for simple first-order reactions, using the following expression:

$$\alpha = \frac{1}{c}\int_{T_0}^{T} \Delta q \mathrm{d}T \tag{10}$$

The normalisation constant c, which is equal to the total heat output during the reaction, is given by:

$$c = \int_{T_0}^{T_1} \Delta q \mathrm{d}T \tag{11}$$

where T_1 is the temperature at the end of the reaction.

Eqs. (7) and (9) are sufficient for the analysis of non-isothermal kinetic data collected using either

DSC of TRPD. They contain no limiting assumptions and can be used with any appropriate rate equation.

4. Implementation of the new method

Two factors are crucial for the correct implementation of the above expressions: the choice of rate equation and the determination of the reaction onset temperature.

4.1. Choice of rate equation

The choice of the correct form of the rate equation is of the utmost importance since the results of any data analysis depend upon the rate equation used. Two methods can be used to distinguish between different models: the first involves directly comparing the observed degree of reaction curves with curves calculated using each model and the second involves considering the linearity of a ln–ln plot, using either Eqs. (7) and (9), for each model.

Reaction curves are usually non-linear and comparing them directly with curves calculated from rate equations requires curve fitting by optimisation of a number of parameters including: the pre-exponential factor, the activation energy and the reaction onset temperature. It is often difficult to reach a global best fit between these curves. This introduces uncertainties into the measure of the goodness of fit and the values of the refined parameters. A ln–ln plot must be linear if the activation energy is a constant. Any deviation from linearity implies an inappropriate rate equation. Thus, the 'correct' rate equation will always give a completely linear ln–ln plot. For this reason a ln–ln plot provides the most reliable method of deciding on the most appropriate rate equation.

In determining the similarity of data and values calculated using a particular model the whole of the data range must be used. Close similarity between a model and the measured degree of reaction, or linearity of a ln–ln plot, over a limited interval is not sufficient to prove the appropriateness of that model. For example, Fig. 1 contains plots of reaction curves calculated from two models $f_s(\alpha)$ and $f_e(\alpha)$, which are sigmoidal and exponential, respectively. $f_s(\alpha)$ is equal to $f(\alpha)$ of the Avrami equation and $f_e(\alpha)=\ln(\alpha)$ (Table 1). Between the limits a and b the two models

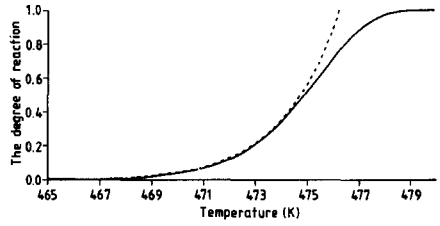

Fig. 1. The degree of reaction curves calculated from sigmoidal (———) and exponential (- - -) rate equations.

predict the same values of the degree of reaction. However, the values of $f_s(\alpha)$ and $f_e(\alpha)$ are completely unrelated even between these limits. If $f_s(\alpha)\neq f_e(\alpha)$ then by Eq. (1), $k_e\neq k_s$. This will affect the values of A and E determined using Eq. (7). The correct value of the activation energy can only be determined using a rate equation proportional to the correct rate equation. In this case the constant of proportionality will be absorbed into the value of the pre-exponential factor. Any non-proportionality will cause the gradient of a ln–ln plot to become non-linear. This makes determination of the activation energy impossible. Calculation of activation energies from non-linear ln–ln plots [1,16,17] cannot lead to reliable results.

4.2. Determination of the reaction onset temperature

The reaction onset temperature (T_0) is the temperature at which the reaction actually starts. This quantity is difficult to measure from non-isothermal data since it involves only a small change in the property being followed and so depends on the sensitivity of the method used for measurement. Knowledge of the temperature at which a reaction starts is necessary for making a ln–ln plot.

The reaction onset temperature can be found by minimising the absolute value of the intercept of a plot of the measured degree of reaction versus the degree of reaction calculated using an estimated value for the reaction onset temperature (T'). An expression for the degree of reaction in terms of the reaction onset temperature, the activation energy and the pre-exponential factor can be obtained by rearranging Eq. (5). For the specific case of the Avrami equation: $\alpha=1-\exp[-(k(T-T_0)/b)^n]$. A ln–ln plot is used to determine values of A and E for the measured values of α assuming that the reaction onset temperature is

equal to T'. Values of the degree of reaction, $\alpha_{calc.}$, can then be calculated for each temperature (T) at which a measured value of α exists. The intercept of a plot of $\alpha_{calc.}$ versus α is the point where $\alpha=0$. At this point, $T=T'=T_0$, so for the Avrami equation, $\alpha=1-\exp[-(k(T'-T_0)/b)^n]$. If the intercept is non-zero then in general, $(T'-T_0)\neq 0$ and T' is not equal to the correct value of T_0. By minimising the absolute value of the intercept of a plot of $\alpha_{calc.}$ versus α, the value of T_0 can be determined. So the following procedure can be used to find the reaction onset temperature:

1. An initial guess is made for the reaction onset temperature from the measured degree of reaction curve. A suitable value is the temperature at which the degree of reaction is first observed to increase from zero.
2. A ln–ln plot is made to determine initial values for the pre-exponential factor and the activation energy.
3. A series of values of the degree of reaction, $\alpha_{calc.}$, are calculated.
4. A plot of $\alpha_{calc.}$ versus α is made and the intercept and gradient are measured.
5. The minimum absolute value of the intercept of the $\alpha_{calc.}$ versus α plot is found by varying the reaction onset temperature.
6. This value of T_0 is then used for making a final ln–ln plot from which final values of A and E are determined.

Since A and E must be recalculated for each new estimate of T_0, an efficient method of minimisation should be chosen, for example Brent's Method [18]. If the appropriate rate equation has been used, then the gradient of the $\alpha_{calc.}$ versus α plot should be equal to unity during the whole procedure.

5. Experimental

In order to illustrate the use of the above method we present an analysis of data collected as part of a simultaneous DSC and TRPD study of the transformation between phases I and II of ammonium chloride.

TRPD data were collected using the energy-dispersive powder diffraction (EDPD) facility at the Daresbury Laboratory Synchrotron Radiation Source (SRS) [19]. The SRS operates at 2 GeV with typical electron beam currents of about 200 mA. The EDPD facility is situated 15 m from the tangent point and benefits from radiation emitted from two poles of a superconducting wiggler magnet of peak field 5 T. The facility receives useful X-ray flux from about 5 keV to about 50 keV with a peak intensity of about 7×10^{11} photons/s mm^2 in a 0.1% bandwidth at 10 keV. The EDPD method uses a polychromatic beam of X-rays and a solid state detector set at a fixed scattering angle, which in this case was about 5°. The fixed geometry makes it straightforward to obtain good quality spectra, in a few seconds, from a sample contained in the DSC with little or no contamination from the sample can or case. The EDPD method has the disadvantage that the momentum resolution is an order of magnitude worse than that obtained using monochromatic techniques. In this case the constrained geometry and the required speed of data collection made EDPD the method of choice.

A 'Linkham Scientific' differential scanning calorimeter [20] was used to make the DSC measurements. This device has the advantage that it can be used at the EDPD facility at Daresbury laboratory to make simultaneous DSC and TRPD measurements. The calorimeter consists of a silver heating block, which encloses the sample container, a resistance heater and temperature and heat flux sensors, contained within a controlled environment case. X-rays enter and leave the cell through thin plastic windows in the casing. Samples were contained in standard DSC sample cans, made from two 7 mm diameter aluminium cups that were crimped together to give a sealed container, modified by the addition of mica windows, one in each half, to allow the transmission of X-rays. Good thermal contact between the sample containers and the heating block was ensured by a spring which held the containers in place. The sample containers contained a few hundredths of a gram of analytical grade ammonium chloride which had been obtained from BDH limited and then ground to a fine powder under liquid nitrogen.

Simultaneous TRPD (Fig. 2) and DSC (Fig. 3) data were collected while heating at 10°min^{-1}. Diffraction patterns were collected for 10 s each during heating. Further DSC data were collected at constant heating rates of 5, 10, 15, 20 and 25 degrees per minute.

The degree of reaction was determined from the TRPD data by combining and normalising the areas under the (200) reflection from phase I and the (110)

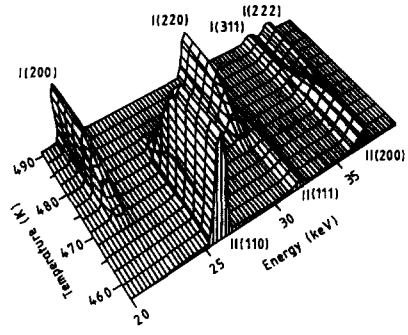

Fig. 2. A 3-d plot made from a series of energy-dispersive powder diffraction patterns collected during the transformation of a sample of ammonium chloride from phase II (Fm3m) to phase I (Pm3m) while heating at 10°/min.

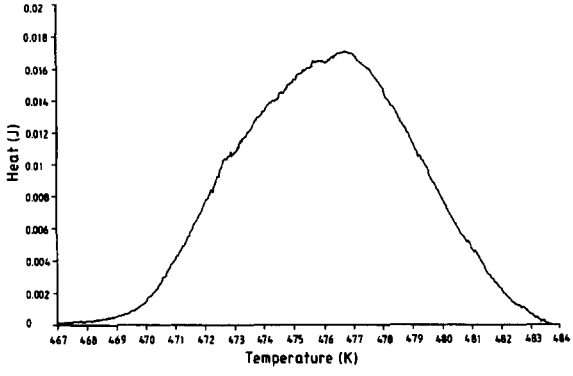

Fig. 3. A DSC trace collected during the transformation of a sample of ammonium chloride from phase II (Fm3m) to phase I (Pm3m) while heating at 10°/min.

reflection from phase II for each of the powder diffraction patterns. Peak areas were determined using a profile fitting method [21].

An estimate for the reaction onset temperature of 465 K was made by inspection of the measured degree of reaction curve (Fig. 6). Initial ln–ln plots (Fig. 4) were made, using Eq. (7), for each of the rate equations in Table 1. Values of the activation energy calculated from these plots are contained in Table 2. Plots made using the Avrami equation were found to come closest to a straight line so this equation was used for subsequent analysis using both the new method and the methods previously reported.

The DSC data were integrated and normalised using Eqs. (10) and (11) (Fig. 5). ln–ln plots were prepared using Eq. (9) with the Avrami equation. Plots were made for various temperatures and had an average gradient of 2 (Table 3).

Table 2
Approximate values of the activation energy (E) calculated for various integrated rate equations from plots using Eq. (7)

Form of integrated rate equation	E (kJ/mol)
Power law	2000
Contracting area	800
Contracting volume	800
Diffusion (1-D)	1000
Diffusion (2-D)	2000
Diffusion (3-D)	2000
Avrami (n=2)	400
Avrami (n=3)	200
Avrami (n=4)	100

The reaction onset temperature was refined, starting from the value of 465 K, using the procedure described in Section 4 above, with n=2 in the Avrami equation. The final value of the reaction onset temperature was found to be about 460 K. The reaction onset temperature could not be refined using any of the other rate equations since they did not give linearc ln–ln plots. A further ln–ln plot was made using the data collected at 10°/min, to give a final value for the activation energy (Table 4). There was found to be close agreement between the observed degree of

Table 3
Values for n and goodness of fit (χ^2) determined from DSC data from plots using Eq. (9)

Temperature (K)	n	χ^2
475	1.8(3)	1.5
477	2.4(3)	0.88
479	2.1(4)	0.64
481	1.9(6)	0.46
482	1.8(7)	0.32
483	1.7(7)	0.25

Table 4
Values for the activation energy (E), pre-exponential factor (A), and goodness of fit (χ^2) determined from TRPD and DSC data from plots using Eq. (7)

Type of data	E (kJ/mol)	ln A (ln s^{-1})	χ^2
TRPD	400(80)	100(20)	0.17
DSC	450(90)	110(25)	0.18

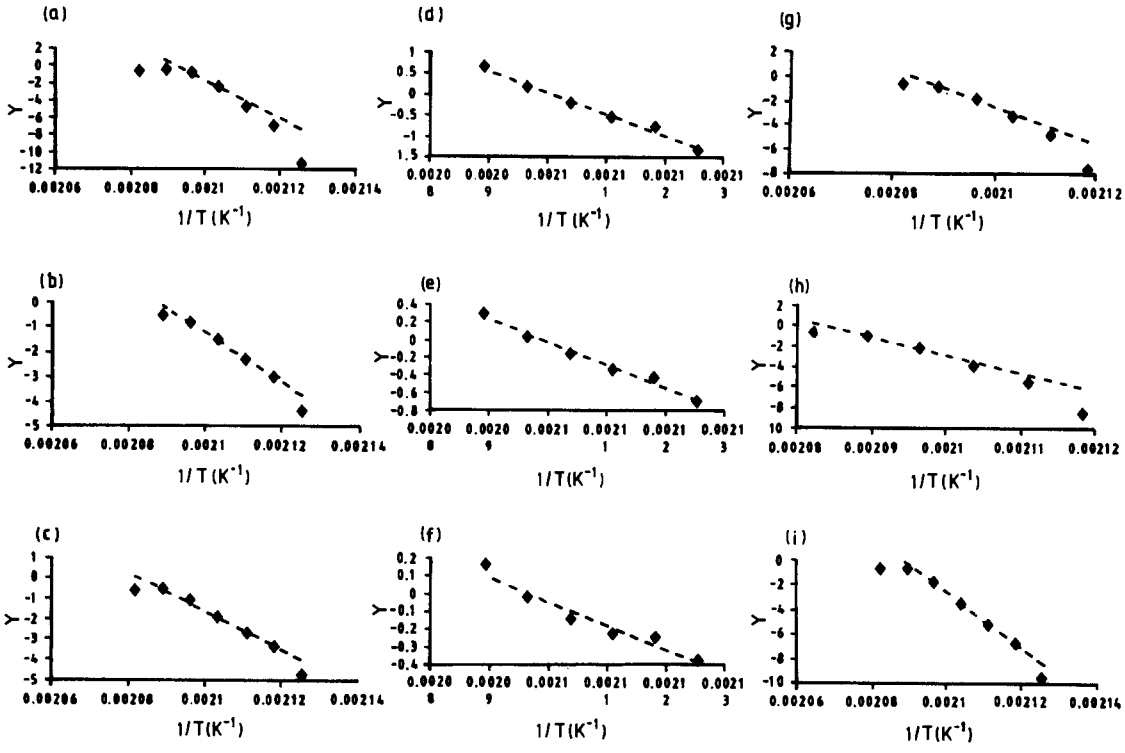

Fig. 4. Plots of ln–ln made using Eq. (7) and the rate equations contained in Table 1: (a) Exponential law; (b) Contracting area; (c) Contracting volume; (d, e, f) Avrami (n=2, 3, 4); (g, h, i) 1-D, 2-D and 3-D diffusion. In each case $Y=\ln[bf(\alpha)/(T-T_0)]$. The activation energies contained in Table 4 were calculated from the gradients of the dashed lines.

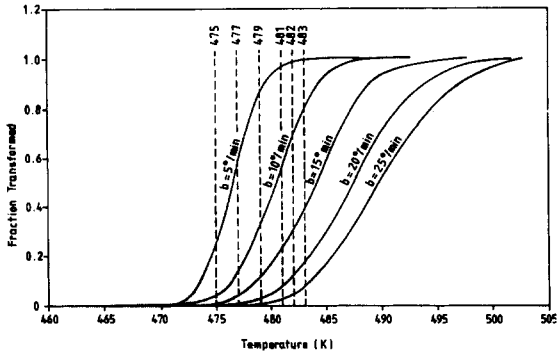

Fig. 5. The fraction of ammonium chloride transformed for various heating rates (b) determined by integration and normalisation of data collected using DSC. Values of the fraction transformed were determined for each heating rate at 475, 477, 479, 481, 482 and 483 K and used with Eq. (9) to determine the values of n contained in Table 3.

reaction curve and the curve calculated using the Avrami equation with these parameters (Fig. 6).

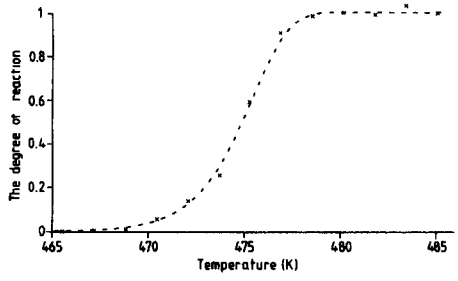

Fig. 6. The degree of reaction curve determined from TRPD data (x x x x) together with the curve calculated using the Avrami equation with n=2 (- - -).

6. Results and discussion

We have shown that the new method of analysis can be used to determine which rate equation best describes a particular reaction or transformation. In this case it was found that the transformation was best described by the Avrami equation.

The reaction onset temperature was found to be about 460 K by adjusting the intercept of an $\alpha_{calc.}$ versus α plot to be as close to zero as possible. This is slightly higher than the values of 456.25 K [22] and 457.65 K [23] that have previously been reported for the equilibrium transition temperature as would be expected for a non-zero heating rate.

The new method was also used to determine a value of 2 for n from the DSC data, and values of the activation energy and pre-exponential factors from both TRPD and DSC data (Table 4). Activation energies were found from the TRPD data using the Avrami equation with n equal to 2, 3, and 4. Calculated curves using each of these values matched the measured degree of reaction curve equally well. This confirms that a value for n cannot be found from a single non-isothermal measurement [24].

The values found for the activation energy might at first sight seem rather large. It must be remembered that this is the activation energy per mole. In this case the energy of activation probably corresponds to a mole of nucleation sites. The transformation mechanism suggested by n being equal to 2 could be either one-dimensional growth of crystals, or very rapid nucleation followed by two-dimensional growth [1]. Previous microscopic studies [25] support the latter mechanism.

The activation energies determined using the new method are in agreement with each other but not with the value of E=213(15) kJ mol^{-1} found using the isothermal method [23]. The cause of this disagreement is that the value of n determined using the isothermal method was 3. The new method used with n set equal to 3 gave a value of 210(30) kJ mol^{-1} for the activation energy which is in close agreement with that determined using the isothermal method. Values for n are determined from isothermal data using either curve fitting [23] or a Sharp–Hancock analysis [26]. Both these methods rely on using data collected at the beginning and end of the transformation which tends to be less reliable than that collected in the middle section. The non-isothermal method has the advantage that heating rates can be chosen so as to give maximum overlap of the temperature ranges of the middle sections of reactions occurring at different heating rates. Since, using the non-isothermal method, n is determined at constant temperature, measurements can be made without reference to values at the extremes of the reaction curve.

Activation energies calculated using other rate equations were found to be at least twice as large as those found when using the correct form of the rate equation (Table 2).

Some of the previous methods available for non-isothermal data analysis were used to find values for the activation energy and pre-exponential factor from the TRPD and DSC degree of reaction curves (Tables 5 and 6). Values of A were calculated where possible using each method. Estimates for the goodness of fit, χ^2, have been included as indications of the linearity of the plots [18]. The rate equation method, using the Avrami equation with n=2, gave values similar to the new method when used with the TRPD data, but these were different to the values obtained using the DSC data. The rate equation method, however, gave ln–ln plots that were inferior to, and therefore less reliable than, those obtained using the new method. The other methods failed to give results that were consistent and generally, did not give agreement with the observed degree of reaction curves.

Table 5
Values for the activation energy (E), pre-exponential factor (A), and goodness of fit (χ^2) determined from TRPD data using the methods of analysis mentioned in the text

Method	E (kJ/mol)	ln A (ln s^{-1})	χ^2
CRSS (1)	1190(70)	—	0.82
CRSS (2)	600(30)	310(20)	0.81
Rate equation	460(90)	110(24)	0.72

Note: CRSS (1) denotes the Coats–Redfern–Sestak–Satava method with the assumption that $E/RT \ll 1$. CRSS (2) denotes the same method with the assumption that $E/RT \gg 1$.

Table 6
Values for the activation energy (E), pre-exponential factor (A), and goodness of fit (χ^2) determined from DSC data using a selection of methods of analysis

Method	E (kJ/mol)	ln A (ln s^{-1})	χ^2
CRSS (1)	1700(200)	—	0.14
CRSS (2)	900(100)	220(40)	0.074
Rate equation	700(200)	180(50)	2
Takhor	60(20)	120(29)	0.27
Kissinger	42(2)	—	6.8
Augis–Bennett	30(20)	17(10)	0.95

Note: CRSS (1) denotes the Coats–Redfern–Sestak–Satava method with the assumption that $E/RT \ll 1$. CRSS (2) denotes the same method with the assumption that $E/RT \gg 1$.

The goodness of fit parameters obtained using the Coats–Redfern–Sestak–Satava method were found to be very small when the assumption that $E/RT \gg 1$ was made. However, the values for E obtained were much larger than those obtained using the other methods. During the derivation of the CRSS method the assumption that $T_0 \ll T$ is made. The new method gives values for the activation energy of a similar magnitude to those obtained using the CRSS method with $E/RT \gg 1$ when the reaction onset temperature is set to zero. So, even though the CRSS method in this case gives the straightest line the assumption that $T_0 \ll T$ leads to the wrong value of the activation energy.

7. Conclusions

We have presented a method suitable for the analysis of non-isothermal data collected using either DSC or TRPD. The method allows the correct rate equation to be found, the reaction onset temperature to be calculated and gives values for other parameters such as the energy of activation. Our analysis suggests that the values of the activation energy calculated using previous methods tend to be too large.

Results obtained using the non-isothermal method are of a similar accuracy to those calculated using isothermal methods, but the non-isothermal method has important advantages over the isothermal method. One non-isothermal run can yield all the relevant information if the reaction mechanism is a simple one, and the problems associated with reaching isothermal temperatures before the onset of the reaction are avoided. Values of other parameters, such as n in the case of the Avrami equation, are more reliably determined since they can be found from ln–ln plots using Eq. (9) at a large number of temperatures. This means that the lower quality data measured at low degrees of transformation need not be used.

This new method provides a common framework for the analysis of data collected in kinetic studies using both TRPD and DSC. The use of this method will allow comparison of the results of different investigations and forms the basis for detecting mechanistic differences between processes.

Acknowledgements

We would like to thank Mr. W. Bras and Mr. B.E. Komanschek for loan of the Linkham Scientific DSC, Mr. D. Bogg for assistance with the DSC electronics, Mrs. V.C. Matthews and Mrs Mandy Todd for drawing the figures, and Dr. J. Anwar for stimulating discussions.

References

[1] C.H. Bamford, C.F.H. Tipper (Eds.), Comprehensive Chemical Kinetics, Vol. 22, Elsevier, New York, 1980, Ch. 3.
[2] S. Arrhenius, Zeitschrift fur Physicalische Chemie 226 (1889) 226.
[3] H.E. Kissinger, J. Res. NBS 57 (1956) 217.
[4] J.A. Augis, J.E. Bennett, J. Thermal Anal. 13 (1978) 283.
[5] R.L. Takhor, Advances in nucleation and crystallization of glasses, Am. Ceram. Soc., Columbus, 1972, p. 166.
[6] A.W. Coats, J.P. Redfern, Nature 201 (1964) 68.
[7] J. Sestak, Thermochim. Acta 3 (1971) 150.
[8] V. Satava, Thermochim. Acta 2 (1971) 423.
[9] M. Avrami, J. Chem. Phys. 7 (1939) 1103.
[10] M. Avrami, J. Chem. Phys. 8 (1940) 212.
[11] M. Avrami, J. Chem. Phys. 9 (1941) 177.
[12] W.A. Johnson, K.F. Mehl, Trans. AIME 135 (1939) 416.
[13] B.V. Erofeev, N.I. Mitskevich, Reactivity of Solids, Elsevier, Amsterdam, 1961, p. 273.
[14] H. Yinnon, D.R. Uhlmann, J. Non-Crystalline Solids 54 (1983) 253.
[15] T. Ozawa, Polymer 12 (1971) 150.
[16] K. Rajeshwar, Thermochim. Acta 45 (1981) 253.
[17] T.A. Clarke, J.M. Thomas, Nature 219 (1968) 1149.
[18] W.H. Press, S.A. Teukolsky, W.T. Vetterling, B.P. Flannery, Numerical Recipes in C: The Art of Scientific Computing, 2nd edn., Cambridge University Press, Cambridge, 1992, p. 404.
[19] S.M. Clark, Nucl. Instrum. Methods A 276 (1989) 381.
[20] W. Bras, G.E. Derbyshire, A. Devine, S.M. Clark, J. Cooke, B.E. Komanschek, A. Ryan, J. Appl. Cryst. 28 (1995) 26.
[21] S.M. Clark, J. Appl. Cryst. 28 (1995) 646.
[22] J. Poyhonen, J. Ann. Acad. Sci. Fenn. A VI 58 (1960) 1.
[23] S.M. Clark, E. Doorhyee, J. Phys.: Condens. Matter 4 (1992) 8969.
[24] T.J.W. De Bruijn, W.A. De Jong, P.J. Van der Berg, Thermochim. Acta 45 (1981) 315.
[25] A.P. Chupakhin, A.A. Sidel'nikov, V.V. Boldyrev, React. Sol. 3 (1987) 1.
[26] J.D. Sharp, J.H. Hancock, J. Am. Ceram. Soc., 55 (1972) 74.